Micro–Computed Tomography Evaluation of ProTaper Next and BioRace Shaping Outcomes in Maxillary First Molar Curved Canals

Damiano Pasqualini, DDS, Mario Alovisi, DDS,* Andrea Cemenasco, BSc,† Lucia Mancini, PhD,‡ Davide Salvatore Paolino, MS, PhD,§ Caterina Chiara Bianchi, MD,† Andrea Roggia, DDS,* Nicola Scotti, DDS,* and Elio Berutti, MD, DDS**

Abstract

Introduction: The aim of this micro–computed tomography study was to describe the shaping properties of ProGlider/ProTaper Next (PG/PTN) and ScoutRace/BioRace (SR/BR) nickel-titanium rotary systems. **Methods:** Thirty maxillary first permanent molars were selected. Mesiobuccal canals were randomly assigned (n = 15) to PG/PTN or SR/BR groups. Irrigation was performed with 5% NaOCl and 10% EDTA. Specimens were scanned (voxel size, 9.1 μm) for matching volumes and surface areas and post-treatment analyses. Root canal centering ability, canal geometry enlargement, and thickness of dentinal wall at inner curvature were assessed at apical level and point of maximum curvature. Results were analyzed with 4 one-way analyses of variance. **Results:** Canal centering ability was superior in PG/PTN (P = .006 at apical level, P = .025 at point of maximum curvature). PG/PTN demonstrated a more conservative increase of canal areas (P = .027 at apical level, P = .038 at point of maximum curvature). Centrifugal increase in canal diameters did not significantly differ between groups (P = .65 at apical level, P = .61 at point of maximum curvature). Inner dentinal wall thickness was less reduced with PG/PTN compared with SR/BR, with no statistical differences (P = .23 at point of maximum curvature, P = .89 at apical level). PG/PTN shaping taper ranged between 6% and 7%. **Conclusions:** Neither system produced significant shaping errors in curved canals. PG/PTN system showed better preservation of canal anatomy. PTN offset section did not influence final preparation taper. *(J Endod 2015;41:1706–1710)*

Key Words

BioRace, canal shaping, canal transportation, micro-CT, NiTi rotary instrument, ProTaper Next

The introduction of nickel-titanium (NiTi) instruments has led to safer, easier, and less invasive preparation of canals with preservation of the original canal anatomy (1–7). The ProTaper Next (PTN) rotary system exhibits M-wire technology, whose properties allowed to reduce the number of instruments necessary to shape even extremely curved and narrow canals (6–11). The instruments are characterized by an offset centered rectangular cross section that gives the files a characteristic swaggering motion during rotation. The taper of PTN instruments refers to the outer profile and not to the progression in section diameters. No data are available concerning the real post-shaping taper. Furthermore, the shaping ability of this system in curved canals has yet to be fully characterized. BioRace system (BR) is a widely diffused file manufactured from conventional austenite NiTi with a triangular cross section and NiTi electropolishing (12, 13).

Micro–computed tomography (micro-CT) has emerged as a powerful tool for *ex vivo* evaluation of root canal morphology because it is accurate as anatomic sectioning (14–18). Micro-CT enables analysis of volume changes, cross-sectional shape, taper, and proportion of prepared surface by matching reconstructed sample volumes of preoperative and postoperative canal systems (19, 20). The primary objective of this *ex vivo* study was to describe shaping outcomes of PTN and BR systems in terms of volume and surface changes, canal centering ability, and canal geometry modification by micro-CT analysis. The secondary objective was to quantify the effect of the swaggering motion on the resulting real taper after shaping with PTN.

Materials and Methods

Maxillary first permanent molars extracted for periodontal disease were used in accordance with approval from the local ethics committee. Study power was set at 80%, and a sample size of 15 specimens per group was calculated (G*Power, Kiel University, Kiel, Germany).

Low-resolution scout scans were performed (21) (450 projections through a 225° rotation, 100 kV, 80 μA) to attain an overall outline of the root canal anatomy.

COBRA 7.2 (Exxim, Pleasanton, CA) software was used to reconstruct the axial slices with an isotropic voxel size of 36 μm. Reconstructed volumes were visualized with VGStudio MAX 2.0 software (Volume Graphics GmbH, Heidelberg, Germany).

Morphologic parameters of the mesiobuccal (MB1) canals were obtained. MB1 canals 12 $\pm$ 2 mm from canal orifice to apical foramen, 25°–40° primary root curvature according to the Schneider method (22), 4 < r $\leq$ 8 mm radius of curvature (23), and a point of maximum curvature located within the middle third of the root canal were

From the *Department of Surgical Sciences, Dental School, Endodontics, University of Turin, Turin; †Department of Radiodiagnostics, University of Turin, Turin; ‡Elettra Sincrotrone Trieste S.C.p.A, Trieste; and §Department of Mechanical Engineering and Aerospace, Politecnico di Torino, Turin, Italy.

Address requests for reprints to Dr Damiano Pasqualini, via Nizza, 230–10126 Torino, Italy. E-mail address: damiano.pasqualini@unito.it

0099-2399/$ - see front matter

http://dx.doi.org/10.1016/j.joen.2015.07.002

used. Teeth with a distinct fourth canal orifice were selected, and those with significant calcifications were excluded.

X-ray Micro-CT Analysis

The selected samples were then scanned at higher spatial resolution (2400 projections through a 360° rotation, 100 kV, 80 μA).

Axial slices were reconstructed with COBRA 7.2 and elaborated for ring artifact reduction by the Pore3D software library (21). Reconstructed axial slices were equalized and converted to TIFF file format with ImageJ (National Institutes of Health, Bethesda, MD) with an isotropic voxel size of 9.1 μm. Each image stack was processed by Amira 5.3.3 (Visage Imaging, Richmond, Australia) for volume registration and cutting plane selection, which was the same for pretreatment and post-treatment samples.

Each root canal path was analyzed with high-resolution three-dimensional (3D) rendering and orthogonal cross sections. Preoperative root canal surface area and volume were collected. Root sections orthogonal to the canal axis were set at 2 different levels, 1 mm from the canal apex (A) and at the point of maximum curvature (C). Axial slices were analyzed with ImageJ to measure area and diameters (major and minor) by using a minimum threshold algorithm to avoid manual errors (24). The major diameter was calculated as the distance between the 2 most distant pixels included in the root canal cross-sectional area; the minor diameter was defined as the longest chord orthogonal to the respective major diameter (25). Measurements were made by an expert operator who was blinded to allocation of specimens.

Final shaping taper of PTN was examined by using high-resolution 3D rendering (Fig. 1). Root sections orthogonal to the canal axis were set with a 1-mm step from apical foramen to canal orifice, and minor diameters were measured.

Specimen Preparation

Forty-five teeth were assessed, and 11 were excluded because of their anatomic features. The remaining 34 teeth were randomly allocated to experimental groups, ProGlider and ProTaper Next (PG/PTN) and ScoutRace and BioRace (SR/BR), and between 2 expert operators by using a computer-generated randomization table. Operators were experienced in both techniques and previously calibrated for pecking speed and pressure on the handpiece. Instruments in both groups were used with in-and-out motion, with no intentional brushing action against canal walls. Because each instrument required a specific technique, it was not possible to blind operators to their allocation. However, randomization, allocation, and statistical analysis were performed by blinded operators.

After access cavity preparation, canal scouting was performed in all specimens with #10 K-file at working length (WL) by using Glyde (Dentsply Maillefer, Ballaigues, Switzerland) as lubricating agent (0.80 mg) (26). WL was established under ×10 magnification (OPMI Pro Ergo; Carl Zeiss, Oberkochen, Germany) when the tip was visible at the apical foramen.

Two specimens from each group required different preflaring and glide path protocols to reach full WL because of their anatomy and were excluded from the study.

In group PG/PTN (n = 15), glide path was performed with PG single file (0.16, .02 to .085) (Dentsply Maillefer) by using X-Smart motor (Dentsply Maillefer) (300 rpm, 4 Ncm) at WL. Root canal shaping was performed with PTN X1 (0.17, .04 to .075) and X2 (0.25, .06 to .07) (Dentsply Maillefer) by using X-Smart (300 rpm, 4 Ncm) at WL.

In group SR/BR (n = 15), glide path was performed with SR system (SR1, 2, and 3; taper .02 and tip size 0.10–0.15–0.20 mm, respectively) (FKG, La Chaux-de-Fonds, Switzerland) by using X-Smart (600 rpm, 1.5 Ncm) at WL. Root canal shaping was performed with BR1 (0.15, .05), BR2 (0.25, .04), and BR3 (0.25, .06) (FKG) by using X-Smart (600 rpm, 1 Ncm) at WL. New sets of instruments were used for each canal in both groups. The duration of instrumentation was recorded for each group.

Irrigation was performed with a 30-gauge needle syringe and alternated 5% NaOCl with 10% EDTA for a total of 10 mL each per specimen (27, 28). Root canals were dried with sterile paper points, and specimens were micro-scanned for post-treatment analysis.

The following parameters were measured in both preoperative and postoperative scans:

1. Root canal volume and surface area
2. Canal gravity center coordinates and shift in millimeters (to assess root canal centering ability); the center of each section was

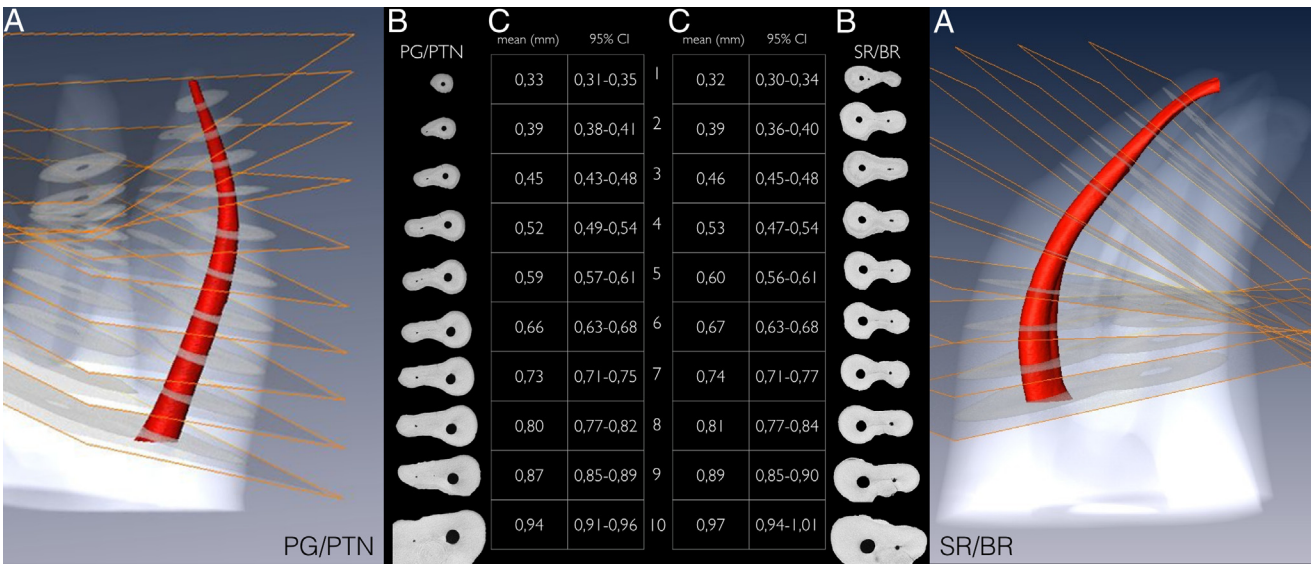

Figure 1. Representative images of ProTaper Next and BioRace post-shaping taper. 3D reconstruction with 1-mm step cutting planes (*A*), images of corresponding axial slices (*B*), and descriptive statistics of minor canal diameters for each slice and relative percentage taper of each step (*C*). CI, confidence interval.

automatically segmented by using ImageJ software before and after instrumentation through the center of mass algorithm, and average canal transportation (d_c) was calculated
3. Ratio of diameter ratios (RDR) and ratio of cross-sectional areas (RA) (to assess symmetrical enlargement of the canal geometry) (15); RDR values closer to 1 correspond to better maintenance of the original canal geometry; RA quantifies the tendency of the instrument to enlarge the root canal space, and values closer to 1 correspond to reduced enlargement
4. Thickness of dentinal wall at inner curvature to evaluate the percent of dentin removal after instrumentation (d_inn)

Parameters were measured at A and C levels of analysis. Shapiro-Wilk normality test was used to analyze data distribution.

Four one-way factorial analyses of variance ($P < .05$) were performed to evaluate the influence of instrumentation on RDR, RA, d_c, and d_inn at each level of analysis (A and C). The Fisher least significant difference procedure was used as a post hoc test. All statistical analyses were performed with Minitab 15 software package (Minitab Inc, State College, PA).

Results

No instrument fractured during canal preparation. Initial mean canal surface areas were 16.611 mm^2 and 16.004 mm^2 ($P = .52$), and initial mean canal volumes were 2.091 mm^3 and 1.934 mm^3 ($P = .64$) in PG/PTN and SR/BR groups, respectively. Statistics of number of pecking motions and time, post-instrumentation canal surface and volume delta values, d_c, RDR, RA, and d_inn at A and C levels of analysis are represented in Table 1.

Figure 2 represents an example matching of preoperative (green) and postoperative (red) shapes in both groups.

Canal centering ability (d_c) was significantly superior in PG/PTN compared with SR/BR ($P = .006$ at A, $P = .025$ at C).

Both systems demonstrated a homogeneous increase in root canal diameters (RDR) at the points of analysis in each direction ($P = .65$ at A, $P = .61$ at C). PG/PTN demonstrated more conservative enlargement of the root canal areas (RA) at both points of analysis compared with SR/BR ($P = .027$ at A, $P = .038$ at C).

On average, PG/PTN reduced the inner dentinal wall thickness (d_inn) at C (−11.2%) to lesser extent than SR/BR (−17.96%). However, this was not statistically significant ($P = .23$). No differences were found between groups at A ($P = .89$).

A 3D visualization of a root canal shaped with PG/PTN and SR/BR systems (red) and the shaping outcomes are presented in Figure 1*A–C*. Progression of root canal diameters (1-mm step) from the apical foramen to root canal orifice demonstrates that the real shaping taper ranges from 6% to 7% in the PG/PTN group, coherent with the declared taper of the instrument profile.

Discussion

Previous studies have shown that root canal transportation leads to excessive dentin removal, with high risk of straightening the original canal curvature and ledge formation with less residual thickness of the dentin walls, significantly affecting long-term prognosis (29–31). Evaluation of changes to canal shape after instrumentation is a reliable assessment of the ability of a shaping technique to preserve the original anatomy (3, 9). Studies have demonstrated the value and reproducibility of micro-CT when evaluating shaping outcomes after preparation with different NiTi instruments (15–20). This *ex vivo* study used micro-CT to describe the shaping performances of the PTN and BR systems in curved root canals, following glide path with PG and SR, respectively. Previous studies demonstrated that canal transportation was more pronounced when shaping narrow curved canals than wider canals of maxillary molars (26). Therefore, MB1 root canals were selected. Natural variation in morphology has led to the establishment of measures to ensure comparability of pre-instrumentation geometric parameters (9, 22). This study considered apical and maximum curvature levels of analysis, representing the areas where iatrogenesis and canal aberrations may be easily introduced (29).

Glide path and coronal enlargement are crucial to achieving a more direct path to the apical end of the canal, removing coronal interferences and reducing the number of pecking motions required to reach full WL (30, 32). Previous studies report that the creation of a glide path and preliminary enlargement enhance the performance of PTN instruments, whereas PTN without a glide path results in a higher mean volume of removed dentin (30, 33). PG reduced the stress in PTN X1 and pecking motions required during shaping because of its ability to create a preliminary flaring of the coronal and middle portions of the root canal (30, 33).

The PTN off-centered rectangular cross section gives the file a reduced pattern of contact between the instrument and canal wall (11, 34), providing the swaggering motion during instrument rotation. This feature has been suspected to change instrument envelope of motion, dramatically increasing the final taper of the preparation. The BR system, with a triangular cross-section design and alternating cutting edges, is a validated method with a centered section and a traditional NiTi alloy (10) and shows significantly different characteristics to PTN in terms of instrument design, number of files in the sequence, protocol of use, and duration of instrumentation. Besides instrument dimension, other factors including metallurgical properties, instrument design, and kinematic and instrument use may influence canal transportation (1, 7).

The primary aim of this study was to assess canal preparation outcomes of 2 NiTi rotary systems with equal size and taper (#25, .06) at tip level but different design and sections. Intentional brushing movement was avoided in both systems to eliminate operator-related parameters that are difficult to standardize and that may influence the final taper of the preparation, even inside the same tested group (35). No

TABLE 1. Shaping and 3D/2D Parameters (mean ± standard deviation) Used for Postinstrumentation Analysis in Each Group

Group	Pecking motions	Shaping time (sec)	Δ volume (mm^3)	Δ surface area (mm^2)	Level of analysis	RDR	RA	d_c (mm)	d_inn (%)
PG/PTN	15.4 ± 1.9[a]	32.6 ± 4.9[a]	0.76 ± 0.4	2.81 ± 1.3	M	0.86 ± 0.12	1.53 ± 0.48[a]	0.05 ± 0.03[a]	11.20 ± 10.39
					A	0.93 ± 0.08	1.40 ± 0.37[a]	0.03 ± 0.02[a]	8.81 ± 8.11
SR/BR	21 ± 2.8[b]	36.6 ± 3.5[b]	0.88 ± 0.31	3.06 ± 0.9	M	0.91 ± 0.30	2.23 ± 1.02[b]	0.09 ± 0.05[b]	17.96 ± 15.96
					A	0.90 ± 0.27	2.01 ± 0.89[b]	0.06 ± 0.03[b]	8.41 ± 7.78

A, 1 mm from apical foramen; d_c, average canal transportation by center of gravity shift; d_inn, percentage of dentin thickness removal at inner curve; M, maximum curvature.

Different superscript letters in same column indicate significant differences between groups ($P < .05$). For 2D parameters (RDR, RA, center of gravity shift, percentage reduction in thickness values), significance was compared for same level of analysis (M, A).

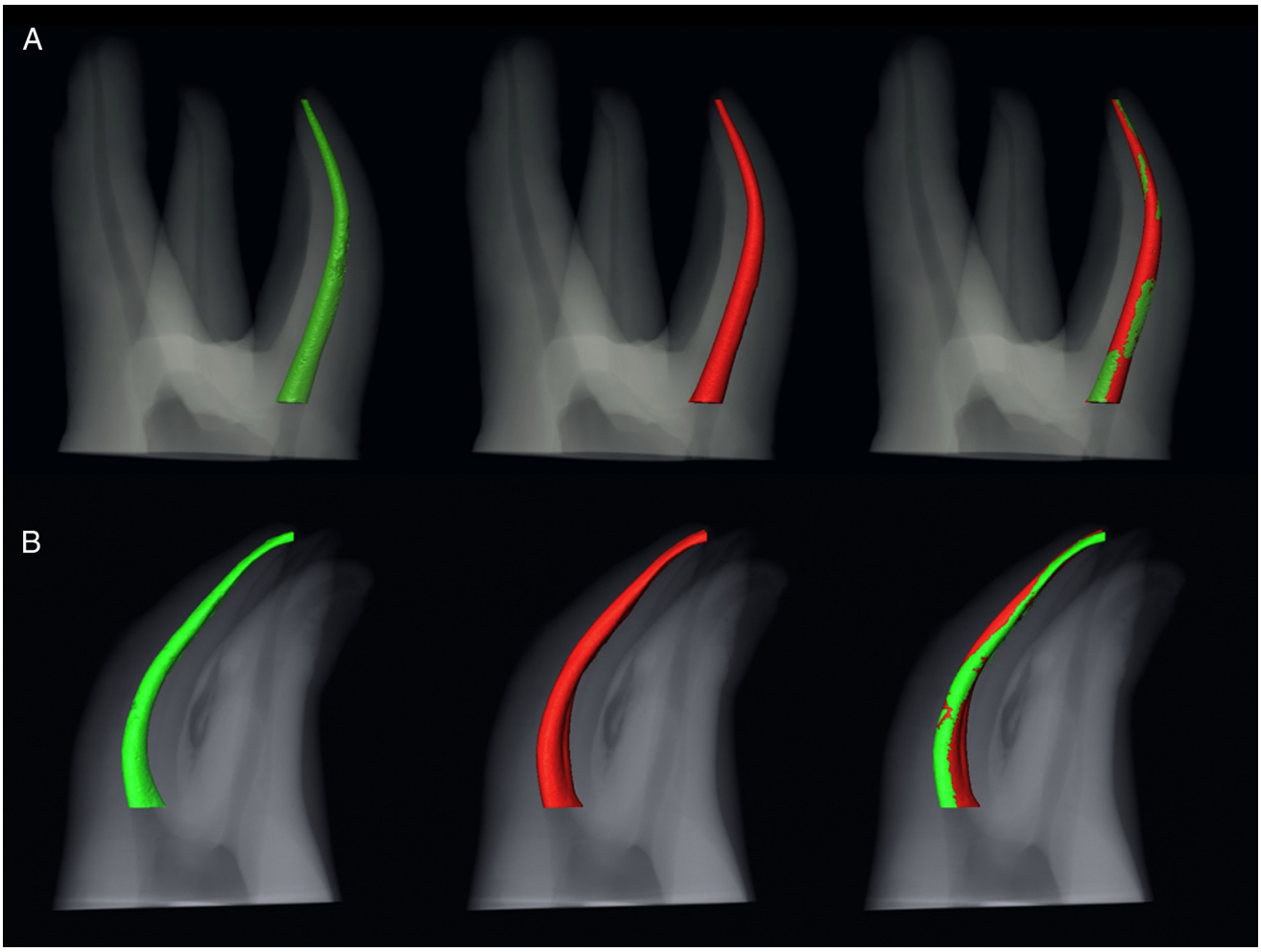

Figure 2. Representative images of matching 3D reconstructions for PG/PTN (*A*) and SR/BR (*B*) groups. *Green* indicates the preoperative volume, and *red* indicates the postoperative volume.

significant differences in post-instrumentation volumes and surface areas were recorded between groups. However, at both A and C, the lowest canal transportation scores were recorded with PG/PTN. Centrifugal increase in canal diameters (RDR) did not significantly differ between groups, whereas PG/PTN demonstrated a more conservative increase of canal areas (RA) and reduction of the inner dentinal wall thickness at point of maximum curvature, probably because of the reduced number of instruments and duration of instrumentation.

The secondary objective of this study was to describe the real final taper of the PG/PTN system root canal preparation. Thus, the analysis aimed to assess the influence of instrument offset section, swaggering movement, and variable taper on the real final taper of the preparation, which was compared with the declared taper of the final shaping instrument (PTN X2). In this study, 3D analysis of the final taper after shaping with PTN X2 demonstrated a homogenous increase in canal taper, ranging from 6% to 7%, which was coherent with the declared taper of the instrument profile.

In conclusion, within the limits of this study, both SR/BR and PG/PTN shaping systems provided root canal preparation without significant shaping errors in maxillary first molar curved canals. The PG/PTN system resulted in a more centered and less invasive preparation. The offset section and swaggering motion of PTN did not appear to enlarge the root canal more than the declared taper of the instrument.

Acknowledgments

The authors thank Dr Nicola Sodini (Sincrotrone Trieste S.C.p.A) for his valuable support in micro-CT analysis and Dr Elisa Bottero (lecturers at the Department of Endodontics, University of Turin Dental School) for active cooperation.

The author Elio Berutti declares financial involvement (patent licensing arrangements) with Dentsply Maillefer for ProGlider instruments. The remaining authors deny any conflicts of interest related to this study.

References

1. Peters OA. Current challenges and concepts in the preparation of root canal systems: a review. J Endod 2004;30:559–67.
2. Hartmann MS, Barletta FB, Camargo Fontanella VR, Vanni JR. Canal transportation after root canal instrumentation: a comparative study with computed tomography. J Endod 2007;33:962–5.
3. Capar ID, Ertas H, Ok E, et al. Comparative study of different novel nickel-titanium rotary systems for root canal preparation in severely curved root canals. J Endod 2014;40:852–6.
4. Haapasalo M, Shen Y. Evolution of nickel–titanium instruments: from past to future. Endod Topics 2013;29:3–17.
5. Capar ID, Arslan H, Akcay M, Uysal B. Effects of ProTaper Universal, ProTaper Next, and HyFlex instruments on crack formation in dentin. J Endod 2014;40:1482–4.

6. Arias A, Singh R, Peters OA. Torque and force induced by ProTaper universal and ProTaper next during shaping of large and small root canals in extracted teeth. J Endod 2014;40:973–6.
7. Elnaghy AM, Elsaka SE. Assessment of the mechanical properties of ProTaper Next nickel-titanium rotary files. J Endod 2014;40:1830–4.
8. Pérez-Higueras JJ, Arias A, de la Macorra JC, Peters OA. Differences in cyclic fatigue resistance between ProTaper Next and ProTaper Universal instruments at different levels. J Endod 2014;40:1477–81.
9. Zhao D, Shen Y, Peng B, Haapasalo M. Root canal preparation of mandibular molars with 3 nickel-titanium rotary instruments: a micro-computed tomographic study. J Endod 2014;40:1860–4.
10. Bürklein S, Mathey D, Schäfer E. Shaping ability of ProTaper NEXT and BT-RaCe nickel-titanium instruments in severely curved root canals. Int Endod J 2015;48:774–81.
11. Capar ID, Arslan H, Akcay M, Ertas H. An *in vitro* comparison of apically extruded debris and instrumentation times with ProTaper Universal, ProTaper Next, Twisted File Adaptive, and HyFlex instruments. J Endod 2014;40:1638–41.
12. Anderson ME, Price JW, Parashos P. Fracture resistance of electropolished rotary nickel-titanium endodontic instruments. J Endod 2007;33:1212–6.
13. Lopes HP, Elias CN, Vieira VT, et al. Effects of electropolishing surface treatment on the cyclic fatigue resistance of BioRace nickel-titanium rotary instruments. J Endod 2010;36:1653–7.
14. Shen Y, Cheung GS. Methods and models to study nickel–titanium instruments. Endod Topics 2013;29:18–41.
15. Pasqualini D, Bianchi CC, Paolino DS, et al. Computed micro-tomographic evaluation of glide path with nickel-titanium rotary PathFile in maxillary first molars curved canals. J Endod 2012;38:389–93.
16. Paque F, Ganahl D, Peters OA. Effects of root canal preparation on apical geometry assessed by micro-computed tomography. J Endod 2009;35:1056–9.
17. Nair MK, Nair UP. Digital and advanced imaging in endodontics: a review. J Endod 2007;33:1–6.
18. Balto K, Müller R, Carrington DC, et al. Quantification of periapical bone destruction in mice by micro-computed tomography. J Dent Res 2000;79:35–40.
19. Peters OA, Laib A, Gohring TN, Barbakow F. Changes in root canal geometry after preparation assessed by high-resolution computed tomography. J Endod 2001;27:1–6.
20. Moore J, Fitz-Walter P, Parashos P. A micro-computed tomographic evaluation of apical root canal preparation using three instrumentation techniques. Int Endod J 2009;42:1057–64.
21. TomoLab X-ray micro-CT laboratory at Elettra–Sincrotrone Trieste S.C.p.A. Available at: www.elettra.trieste.it/lightsources/labs-and-services/tomolab/tomolab.html. Accessed November 23, 2014.
22. Schneider SW. A comparison of canal preparations in straight and curved root canals. Oral Surg Oral Med Oral Pathol 1971;32:271–5.
23. Gu Y, Lu Q, Wang P, Ni L. Root canal morphology of permanent three-rooted mandibular first molars: part II—measurement of root canal curvatures. J Endod 2010;36:1341–6.
24. Neves AA, Silva EJ, Roter JM, et al. Exploiting the potential of free software to evaluate root canal biomechanical preparation outcomes through micro-CT images. Int Endod J 2014 Oct 29. http://dx.doi.org/10.1111/iej.12399. [Epub ahead of print].
25. Versiani MA, Pécora JD, Sousa-Neto MD. Microcomputed tomography analysis of the root canal morphology of single-rooted mandibular canines. Int Endod J 2013;46:800–7.
26. Cruz A, Vera J, Gascón G, et al. Debris remaining in the apical third of root canals after chemomechanical preparation by using sodium hypochlorite and glyde: an *in vivo* study. J Endod 2014;40:1419–23.
27. Berutti E, Marini R, Angeretti A. Penetration ability of different irrigants into dentinal tubules. J Endod 1997;23:725–7.
28. Soares JA, Roque de Carvalho MA, Cunha Santos SM, et al. Effectiveness of chemomechanical preparation with alternating use of sodium hypochlorite and EDTA in eliminating intracanal Enterococcus faecalis biofilm. J Endod 2010;36:894–8.
29. Jafarzadeh H, Abbott PV. Ledge formation: review of a great challenge in endodontics. J Endod 2007;33:1155–62.
30. Elnaghy AM, Elsaka SE. Evaluation of root canal transportation, centering ratio, and remaining dentin thickness associated with ProTaper Next instruments with and without Glide Path. J Endod 2014;40:2053–6.
31. Peters OA, Peters CI, Schönenberger K, Barbakow F. ProTaper rotary root canal preparation: effects of canal anatomy on final shape analysed by micro CT. Int Endod J 2003;36:86–92.
32. Berutti E, Paolino DS, Chiandussi G, et al. Root canal anatomy preservation of WaveOne reciprocating files with or without glide path. J Endod 2012;38:101–4.
33. Berutti E, Alovisi M, Pastorelli MA, et al. Energy consumption of ProTaper Next X1 after Glide Path with PathFiles and ProGlider. J Endod 2014;40:2015–8.
34. Pereira ES, Singh R, Arias A, Peters OA. *In vitro* assessment of torque and force generated by novel ProTaper Next instruments during simulated canal preparation. J Endod 2013;39:1615–9.
35. Alattar S, Nehme W, Diemer F, Naaman A. The influence of brushing motion on the cutting behavior of 3 reciprocating files in oval-shaped canals. J Endod 2015;41:703–9.